

RAPID COMMUNICATION

Adsorption characteristics of arsenic and phosphate onto iron impregnated biochar derived from anaerobic granular sludge

Myeong Eun Lee, Pilyong Jeon, Jong-Gook Kim, and Kitae Baek[†]

Department of Environmental Engineering and Soil Environment Research Center, Chonbuk National University,
567 Baekje-daero, Deokjin, Jeonju, Jeollabukdo 54896, Korea
(Received 21 November 2017 • accepted 28 March 2018)

Abstract—Biological wastewater treatment produces biowaste (sludge), which contains a high portion of organic matter. The organic matter comes from microorganisms, and the biowaste can be converted into biochar, a carbon-rich, fine-grained, and porous substance. Granular sludge from upflow anaerobic sludge blanket contains more organic matter (80 wt% of dry matter) and carbon content (>50% of organic matter). In this study, iron impregnated biochar was prepared to remove arsenic (As) and phosphate, oxyanionic pollutants, from the aqueous phase. The iron impregnation of biochar was executed in a one-step by pyrolyzing the biowaste in the presence of Fe instead of conventional two-step, i.e., biochar production after then modification. The granular sludge biochar and activated sludge biochar did not adsorb at all As and phosphate. The adsorption capacity of granular sludge biochar was enhanced via iron impregnation, and the iron-impregnated granular sludge biochar removed 10.37 mg PO₄³⁻/g, 11.5 mg As(V)/g, and 6.1 mg As(III)/g, respectively. Therefore, the one-step process enhanced the adsorption capacity and reduced processing time for the adsorbent synthesis.

Keywords: Biochar, Phosphorous, Arsenic, Adsorption, Impregnation

INTRODUCTION

Organic wastes have been issued environmentally since the ocean dumping was banned [1]. In the Republic of Korea, more than 100,000 tons of organic waste is being generated per year, of which more than 60,000 tons (58%) is sewage sludge [2]. The sludges, one of the organic wastes, are generated in biological wastewater treatment facilities, and several attempts have been made to treat or recycle the sludge [3-5]. Sludge is divided into three categories: aerobic, anaerobic, and anaerobically digested sludge. Aerobic sludge is produced from the activated sludge process operated under aerobic condition, which is generally treated in an anaerobic digester, and anaerobically digested sludge is a residual sludge after anaerobic digestion. The anaerobic sludge is generated from the anaerobic treatment process operated under anaerobic conditions, and upflow anaerobic sludge blanket (UASB) is one of the anaerobic treatment processes. The sludge produced from the biological wastewater treatment process has a high organic content, and this organic material is mostly composed of microorganisms.

The sludge is one of biomass, which can be converted to biochar via the pyrolysis under little or no oxygen condition [6,7]. Biochar has high carbon content, fine-grained, large surface area of the porous structure, and carbon negative effect to reduce or save carbon [8-10]. In addition, biochar has an excellent capacity to adsorb organic pollutants or heavy metals in soil and water [11,12]. Surface modification is a common choice to enhance the adsorption capacity, especially, iron with strong affinity to anions has been used to in-

crease the adsorption capacity for oxyanionic pollutants [13-17]. However, biochar has been modified after biomass is pyrolyzed, which means that two-step processes are required to prepare modified or impregnated biochar. Even though the modification is effective to enhance the adsorption capacity, the modification of biochar requires additional energy based on the thermal treatment [14-17]. Therefore, a simple process to modify the biochar is needed.

Arsenic (As), one of most toxic anionic pollutants in the water system, threatens humans and the ecosystem, and phosphate causes eutrophication [18, 19]. Therefore, pollutants should be discharged to the water stream after appropriate treatment [20-25]. Inorganic As has two different oxidation states in nature: As(III) (arsenite) and As(V) (arsenate). Above pH 2.2, As(V) exists as anionic forms such as H₂AsO₄⁻, HAsO₄²⁻ and AsO₄³⁻. On the other hand, As(III) is neutral from H₃AsO₃, below pH 9.2 [26-30]. Therefore, the adsorption capacity of As(V) is higher than that of As(III) for most iron-based materials and biochar at the range pH of the water system in nature [31].

In this study, granular sludge with a high portion of organic matter produced from UASB was used to prepare biochar, and the biochar was impregnated with iron oxides prepared by one-step pyrolysis to enhance the adsorption capacity of biochar. The adsorption characteristics of As and phosphate onto the biochar were evaluated.

MATERIAL AND METHODS

1. Materials

The biomass (granular sludge) from UASB and dewatered activated sludge were obtained at a food wastewater treatment process located in Jeonju, Jeollabuk-do, Republic of Korea. NaAsO₂ (Sigma-Aldrich, USA), Na₂HAsO₄ (Sigma-Aldrich, USA), KH₂PO₄

[†]To whom correspondence should be addressed.

E-mail: kbaek@jbnu.ac.kr

Copyright by The Korean Institute of Chemical Engineers.

Table 1. Composition of raw sludges and biochars

	Carbon (%)	Nitrogen (%)	Hydrogen (%)	Organic matter (%)	Biochar yield
Granular sludge (GS)	44.1	8.5	7.1	87	
Activated sludge (AS)	10.2	2.8	1.2	38	
Granular sludge biochar	52.3	8.1	4.6		0.60
Activated sludge biochar	12.1	2.7	0.8		0.80

(Junsei, Japan), and FeCl_3 (Kanto Chemical, Japan) were used without further purification.

2. Biochar and Iron Impregnated Biochar

Granular sludge and activated sludge were pyrolyzed at 300 °C for 3 hours in a furnace under nitrogen environment. To prepare iron impregnated biochar (IMB), the granular sludge was pretreated with a solution of 2.25 M FeCl_3 in a 1 : 1 ratio for 2 hours, after then dried at 105 °C for 4 hours. The pretreated biomass was pyrolyzed at 500 °C with a heating rate of 4 °C/min for 3 hours in a furnace under nitrogen environment. Elemental composition of sludges and biochar was analyzed by an elemental analyzer (EA, Fisons, USA), X-ray diffraction spectroscopy (XRD, Panalytical, Holland) was used to identify the structure of the IMB, and to identify the iron on the surface of IMB by scanning electron microscope (SEM, JEOL, Japan).

3. Adsorption of Phosphate and Arsenic

A mass of 0.1 g of IMB was mixed with 45 mg P/L in an overhead shaker (Finepcr, Korea) at 40 rpm. At the desired time interval, the solid was separated from the mixture using a 0.45 µm syringe filter. The concentration of phosphate in the filtrate was measured by UV-VIS spectroscopy (HS-3300, Humas, Korea) [18, 32]. A mass of 0.1 g of IMB was mixed with 30 mL of 50 mg As/L solution of As(III) and As(V) in an overhead shaker (Finepcr, Korea) at 40 rpm. At the desired time interval, the aqueous phase was separated from the solids using a 0.45 µm syringe filter, and the concentration of As in the filtrate was analyzed by an inductively coupled plasma optical emission spectroscopy (ICP-OES 720, Agilent, USA).

Adsorption kinetics of phosphate and As were fitted with pseudo-first-order model (PFO) and pseudo-second-order model (PSO). The PFO is a widely used rate equation for adsorption of solids and liquids, and expressed as follows [33].

$$\ln(q_e - q_t) = \ln q_e + k_1 t$$

The PSO is a rate equation based on chemisorption, and expressed as follows [34,35].

$$\frac{t}{q_t} = \frac{1}{k_2 q_e^2} + \frac{t}{q_e}$$

where q_e , q_t , t , k_1 , and k_2 are adsorbed amounts of target pollutants (i.e., phosphate and As) at equilibrium state (mg/g), adsorbed amounts of target pollutants at any time t (mg/g), time (h), PFO rate constant (/h), and PSO rate constant (g/mg/h).

RESULTS AND DISCUSSION

1. Characteristics of Sludges and Biochars

Elemental composition and organic matter content of two slud-

ges and biochars derived from the sludges are shown in Table 1. The granular sludge contains an 87 wt% of organic matter, and the organic matter consists of 44.1 wt% of carbon and 8.5 wt% of nitrogen; activated sludge has a 38 wt% of organic matter, and the organic matter consists of carbon and nitrogen of 10.2 wt% and 2.8 wt%, respectively. The granular sludge is an anaerobic microbial community, which is the reason for higher organic matter content and more carbon. Activated sludge has relatively high mineral content because of the fine soil particles in the activated sludge process. Granular sludge has higher organic matter content than activated sludge, and thus granular sludge is more suitable biomass for production of biochar [36]. However, because inorganic substances are known to be involved in the adsorption of various pollutants [37], it is expected that the inorganic substances in the activated sludge contribute to the adsorption of target pollutants. The biochar yield through pyrolysis of granular sludge and activated sludge at 300 °C is 0.60,

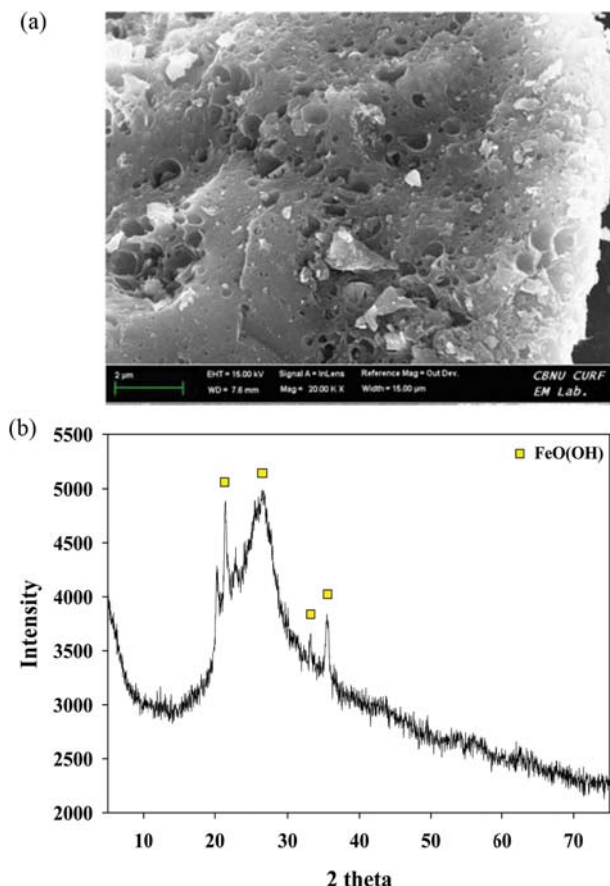


Fig. 1. SEM image (a) and XRD spectra (b) of iron impregnated biochar prepared using granular sludge from UASB process.

0.80, respectively. It is well known that biochar yield increases with the mineral content of biomass [11,38]; therefore, the yield of activated sludge is higher than that of granular sludge. In addition, a significant portion of organic matter in granular sludge is gasified or converted to oil during the pyrolysis. The gas evolution during the pyrolysis helps to generate porous structure in the biochar, and SEM images show the porous structure of IMB (Fig. 1(a)).

XRD analysis shows that iron exists as a form of goethite, expecting that IMB adsorbs efficiently anion pollutants such as phosphate and As (Fig. 1(b)) [39]. To evaluate the amount of iron on the surface of IMB, the IMB was repeatedly washed until no more iron was observed in the washed solution; the amounts of iron in the washed water were analyzed, and the residual iron content was 2.2 mg Fe/g biochar. The granular sludge biochar and activated

sludge biochar did not adsorb at all As and phosphate because the biochar did not have any functional group to adsorb the anionic substances. Even though the biomasses were pyrolyzed at two different temperatures, 300 °C and 500 °C, the biochars did not remove As and phosphate. Therefore, it is required to modify the biochar for the enhancement of the adsorption capacity.

2. Adsorption Kinetics of Phosphate onto IMB

The adsorption of PO_4^{3-} onto the IMB rapidly increases until 10 hours, then gradually increases. After 24 hours, the adsorption of PO_4^{3-} reaches an equilibrium (Fig. 2). When phosphorus exists as a form of PO_4^{3-} in the water, phosphate is adsorbed onto the IMB via the chemical adsorption between iron oxides and PO_4^{3-} . Considering regression coefficient, PSO describes well the adsorption kinetics of PO_4^{3-} (Table 2), which indicates that the adsorption is

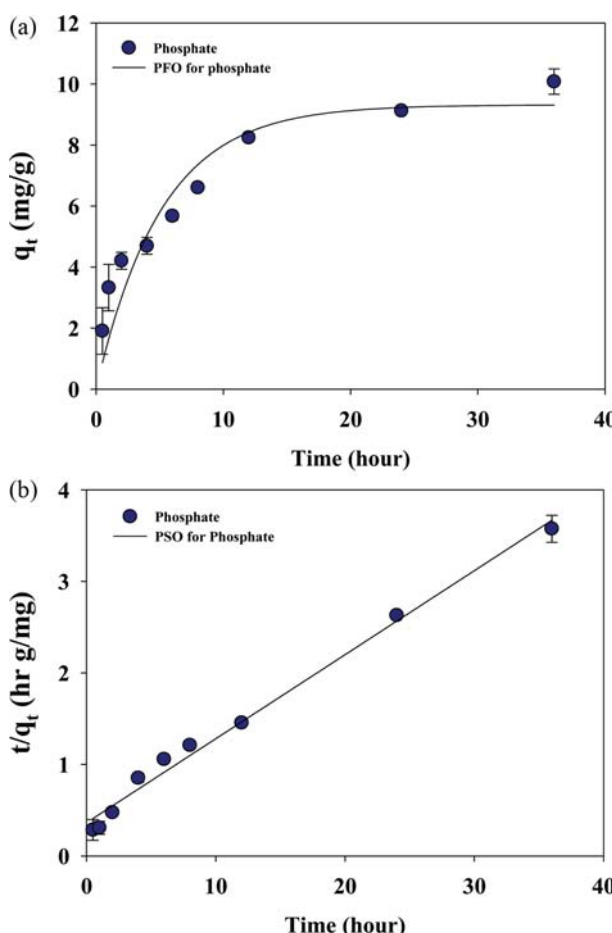


Fig. 2. Adsorption kinetics of phosphorus onto biochar fitted with (a) PFO and (b) PSO kinetic models.

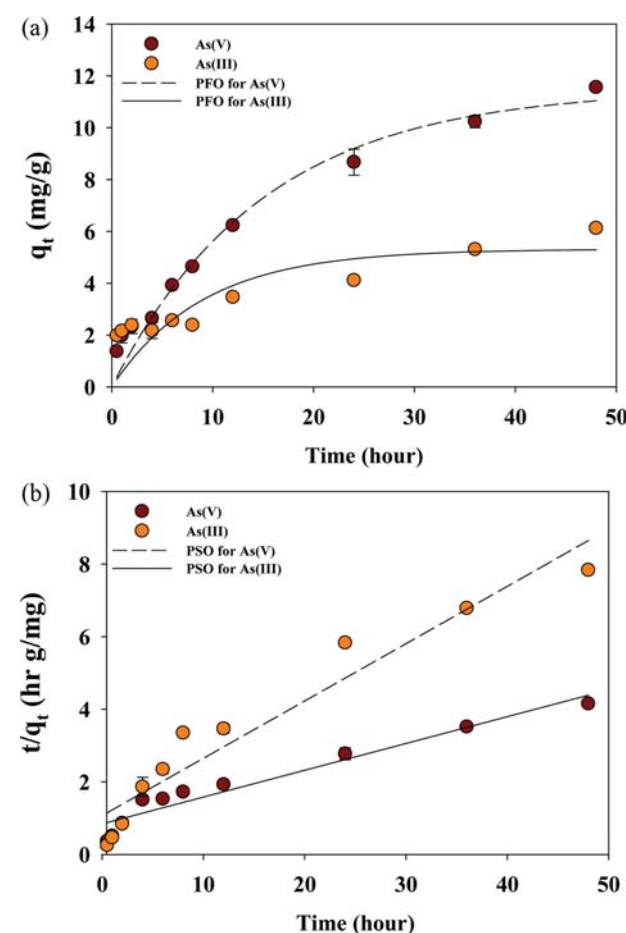


Fig. 3. Adsorption kinetics of As(V) and As(III) onto biochar fitted with (a) PFO and (b) PSO kinetic models.

Table 2. Kinetic parameters for the adsorption of As and phosphorus

	Pseudo-first-order (PFO)			Pseudo-second-order (PSO)		
	k_1 (hr^{-1})	q_e (mg/g)	r^2	k_2 (g/mg/hr)	q_e (mg/g)	r^2
Phosphate	0.194	9.3	0.870	0.0712	10.9	0.987
As(V)	0.067	11.5	0.965	0.0064	13.6	0.938
As(III)	0.111	5.3	0.508	0.0046	6.3	0.927

chemical adsorption because PSO is based on chemisorption [34]. The adsorption capacity of PO_4^{3-} from the adsorption kinetic test was 10.4 mg $\text{PO}_4^{3-}/\text{g}$, which is higher than the adsorption capacities of biochars for PO_4^{3-} reported in the literature [15,40,41]. The biochar treated with ferric oxide on the cotton stalk adsorbed 0.963 mg $\text{PO}_4^{3-}/\text{g}$ [13], and the relatively high adsorption capacity of IMB shows the effectiveness of the IMB to remove phosphorus.

3. Adsorption Kinetics of Arsenic onto IMB

The adsorption kinetics of two As species with different oxidation state was investigated using As(V) and As(III). The adsorption of As(V) increases gradually, after 48 hours reaching 11.5 mg As/g biochar (Fig. 3). Additionally, the pH of the solution was lowered to 3.2 from initial pH of 8.0, which implies that H_2AsO_4^- is a dominant species of As(V). The lower pH results from the release and hydrolysis reaction of ferric from the biochar [42], and the lower pH decrease the adsorption capacity of IMB. The PFO described well the adsorption of As(V) based on the correlation coefficient, indicating that the adsorption is physical adsorption.

The amounts of As(III) adsorbed onto the IMB increased to 6.1 mg As(III)/g, and the equilibrium pH decreased to 3.6 from the initial pH of 8.9 after 48 hours. Considering the equilibrium pH, the dominant species of As(III) is a neutral form. That is the main reason for the lower adsorption of As(III) compared to As(V) because there is no electrostatic interaction between the neutral form of As(III) and IMB [31]. The PSO described well the adsorption of As(III) (Table 2), implying chemical adsorption. On the surface of IMB, As(V) exists as forms of $\equiv\text{FeHAsO}_4^-$, $\equiv\text{FeHAsO}_4^{3-}$, $\equiv\text{FeH}_2\text{AsO}_4$, and $\equiv\text{FeHAsO}_4^{2-}$ and As(III) adsorbs as forms of $\equiv\text{Fe}_2\text{AsO}_3^-$, $\equiv\text{FeH}_2\text{AsO}_3$, $\equiv\text{FeHAsO}_3^-$, $\equiv\text{Fe}_2\text{AsO}_3^{2-}$, and $\equiv\text{Fe}_2\text{HAsO}_3$ [26,43]. Generally, As(V) is adsorbed onto iron oxides surface via chemisorption, and As(III) is removed by physical sorption. Even though the phenomenon is opposite in this study, the regression coefficients are not significantly different, and both models describe the adsorption [44].

The adsorption capacity of IMB for As(V) and As(III) was compared to that of other adsorbents containing iron (Table 3). The less adsorption capacity for As(III) compared to As(V) was observed in other iron oxide materials. Therefore, to improve the adsorption

capacity of the IMB for As(III), additional ways should be considered, including oxidation of As(III) to As(V) other oxidizing materials.

CONCLUSIONS

The adsorption characteristics of As and phosphate by iron-impregnated biochar (IMB) derived from UASB were studied. The granular sludge from UASB has higher content of organic matter and carbon than activated sludge discharged from the same plant. The impregnation was executed in a one-step process by pyrolyzing the biowaste in the presence of Fe. The sludge biochars did not adsorb As arsenic and phosphate because the biochars did not have any functional groups to adsorb oxyanionic As and phosphate. The adsorption capacity of As and phosphate was enhanced by the impregnation of iron, the IMB removed 10.4 mg $\text{PO}_4^{3-}/\text{g}$, 11.5 mg As(V)/g and 6.1 mg As(III)/g for As(III). This result shows that the one-step process of IMB preparation enhances the adsorption capacity of biochar for As and phosphate.

ACKNOWLEDGEMENTS

This research was supported by the Basic Science Research Program through the National Research Foundation of Korea (NRF) funded by the Ministry of Science and ICT.

REFERENCES

- Ministry of Environment, Korea (2010).
- Ministry of Environment, Korea (2011).
- H.-Y. Yoo, *J. Korean Org. Resour. Recycl. Assoc.*, **11** (2016).
- Ministry of Environment, Korea (2014).
- S.-Y. Park, G.-Y. Park, D.-H. Kim, J.-S. Yang and K. Baek, *Sep. Sci. Technol.*, **45**, 1982 (2010).
- E. Agrafioti, G. Bouras, D. Kalderis and E. Diamadopoulos, *J. Anal. Appl. Pyrol.*, **101**, 72 (2013).
- P. Manara and A. Zabaniotou, *Renewable Sustainable Energy Rev.*, **16**, 2566 (2012).

Table 3. Comparison of adsorption capacity for phosphate

Sorbents	Maximum adsorption capacity (mg phosphate/g)	References
Oak tree biochar	0.1	[40]
<i>T. dealbata</i> biochar (500 °C-700 °C)	2.54-4.96	[41]
Granulation of biochar (Bg-FO-1)	0.963	[15]
IMB	10.4	This study

Table 4. Comparison of adsorption capacity for As(V)

Sorbents	Maximum adsorption capacity (mg As/g)	References
$\gamma\text{-Fe}_2\text{O}_3$ composite/biochar	3.2	[13]
Iron oxide amended rice husk char	1.6	[14]
Fe coated rice husk biochar	16.9	[17]
Iron-impregnated biochar (hickory)	2.16	[16]
IMB	11.5	This study

8. J. Lehmann, *Nature*, **447**, 143 (2007).
9. M. Ahmadi, E. Kouhgardi and B. Ramavandi, *Korean J. Chem. Eng.*, **33**, 2589 (2016).
10. P. Jeon, M.-E. Lee and K. Baek, *J. Taiwan Inst. Chem. Eng.*, **77**, 244 (2017).
11. M. Ahmad, A. U. Rajapaksha, J. E. Lim, M. Zhang, N. Bolan, D. Mohan, M. Vithanage, S. S. Lee and Y. S. Ok, *Chemosphere*, **99**, 19 (2014).
12. M. I. Inyang, B. Gao, Y. Yao, Y. W. Xue, A. Zimmerman, A. Mosa, P. Pullammanappallil, Y. S. Ok and X. D. Cao, *Crit. Rev. Env. Sci. Technol.*, **46**, 406 (2016).
13. M. Zhang, B. Gao, S. Varnoosfaderani, A. Hebard, Y. Yao and M. Inyang, *Bioresour. Technol.*, **130**, 457 (2013).
14. C. O. Cope, D. S. Webster and D. A. Sabatini, *Sci. Total Environ.*, **488**, 558 (2014).
15. J. Ren, N. Li, L. Li, J. K. An, L. Zhao and N. Q. Ren, *Bioresour. Technol.*, **178**, 119 (2015).
16. X. Hu, Z. H. Ding, A. R. Zimmerman, S. S. Wang and B. Gao, *Water Res.*, **68**, 206 (2015).
17. A. W. Samsuri, F. Sadegh-Zadeh and B. J. Seh-Bardan, *Environ. Chem. Eng.*, **1**, 981 (2013).
18. D. Kim, K. J. Min, K. Lee, M. S. Yu and K. Y. Park, *Environ. Eng. Res.*, **22**, 12 (2016).
19. H.-S. Yoon, K. W. Chung, C.-J. Kim, J.-H. Kim, H.-S. Lee, S.-J. Kim, S.-I. Lee, S.-J. Yoo and B.-C. Lim, *Korean J. Chem. Eng.*, **35**, 470 (2018).
20. B. K. Mandal and K. T. Suzuki, *Talanta*, **58**, 201 (2002).
21. D. Mohan and C. U. Pittman, *J. Hazard. Mater.*, **142**, 1 (2007).
22. I. Celik, L. Gallicchio, K. Boyd, T. K. Lam, G. Matanoski, X. G. Tao, M. Shiels, E. Hammond, L. Chen, K. A. Robinson, L. E. Caulfield, J. G. Herman, E. Guallar and A. J. Alberg, *Environ. Res.*, **108**, 48 (2008).
23. T. S. Y. Choong, T. G. Chuah, Y. Robiah, F. L. G. Koay and I. Azni, *Desalination*, **217**, 139 (2007).
24. V. H. Smith, *Environ. Sci. Pollut. Res.*, **10**, 126 (2003).
25. C. P. Mainstone and W. Parr, *Sci. Total Environ.*, **282**, 25 (2002).
26. S. Dixit and J. G. Hering, *Environ. Sci. Technol.*, **37**, 4182 (2003).
27. S. M. Miller and J. B. Zimmerman, *Water Res.*, **44**, 5722 (2010).
28. D. Tiwari, A. Jamsheera, Zirlianngura and S. M. Lee, *Environ. Eng. Res.*, **22**, 186 (2017).
29. A. M. Bandpei, S. M. Mohseni, A. Sheikhmohammadi, M. Sardar, M. Sarkhosh, M. Almasian, M. Avazpour, Z. Mosallanejad, Z. Attafar, S. Nazari and S. Rezaei, *Korean J. Chem. Eng.*, **34**, 376 (2017).
30. S.-Y. Shin, S.-M. Park and K. Baek, *Environ. Sci. Pollut. Res.*, **24**, 9820 (2017).
31. S. R. Ryu, E. K. Jeon, J. S. Yang and K. Baek, *J. Taiwan Inst. Chem. Eng.*, **72**, 62 (2017).
32. J.-H. Kim, J.-A. Park, J.-K. Kang, S.-B. Kim, C.-G. Lee, S.-H. Lee and J.-W. Choi, *Environ. Eng. Res.*, **20**, 73 (2015).
33. D. Borah, S. Satokawa, S. Kato and T. Kojima, *J. Hazard. Mater.*, **162**, 1269 (2009).
34. H. Qiu, L. Lv, B. C. Pan, Q. J. Zhang, W. M. Zhang and Q. X. Zhang, *J. Zhejiang Univ.-Sci. A*, **10**, 716 (2009).
35. S. Dawood and T. K. Sen, *Water Res.*, **46**, 1933 (2012).
36. P. Jeon, M.-E. Lee and K. Baek, *J. Taiwan Inst. Chem. Eng.*, **77**, 244 (2017).
37. S.-R. Ryu, E.-K. Jeon and K. Baek, *J. Taiwan Inst. Chem. Eng.*, **70**, 252 (2017).
38. K. B. Cantrell, P. G. Hunt, M. Uchimiya, J. M. Novak and K. S. Ro, *Bioresour. Technol.*, **107**, 419 (2012).
39. J.-C. Lee, E. J. Kim, H.-W. Kim and K. Baek, *Geoderma*, **270**, 76 (2016).
40. Y.-S. Choi, *J. Korean Org. Resour. Recycl. Assoc.*, **23**, 60 (2015).
41. Z. Zeng, S. D. Zhang, T. Q. Li, F. L. Zhao, Z. L. He, H. P. Zhao, X. E. Yang, H. L. Wang, J. Zhao and M. T. Rafiq, *J. Zhejiang Univ.-Sci. B*, **14**, 1152 (2013).
42. J.-C. Yoo, S.-M. Park, G.-S. Yoon, D. C. W. Tsang and K. Baek, *Chemosphere*, **185**, 501 (2017).
43. J. S. Yang, Y. S. Kim, S. M. Park and K. Baek, *Environ. Sci. Pollut. Res.*, **21**, 10878 (2014).
44. E.-K. Jeon, S. Ryu, S.-W. Park, L. Wang, D. C. W. Tsang and K. Baek, *J. Cleaner Prod.*, **176**, 54 (2018).